Strojnícky časopis – *Journal of* MECHANICAL ENGINEERING,
VOL 72 (2022), NO 3, 129 - 140

CONDITIONS FOR LOSS OF STABILITY OF AN AUTONOMOUS VEHICLE DURING A CORNERING MANOEUVRE

MAGDOLEN Ľuboš[1], DANKO Ján[1], MILESICH Tomáš[1], KEVICKÝ Igor[1], HANKO Lukáš[2], SKYRČÁK Robert[1]

[1] Slovak University of Technology in Bratislava, Faculty of Mechanical Engineering, Institute of Transport Technology and Designing, Nám. slobody 17,812 31 Bratislava, Slovakia,
e – mail: lubos.magdolen@stuba.sk
[2] Slovak University of Technology in Bratislava, Faculty of Mechanical Engineering, Institute of manufacturing systems, environmental technology and quality management, Nám. slobody 17,812 31 Bratislava, Slovakia

Abstract: This paper deals with the method of creating a virtual autonomous vehicle dynamics model SimRod in AMESim environment and implementing such a model in Prescan and MATLAB/Simulink environments and performing co-simulation of the vehicle cornering maneuver at different values of the grip factor in these software. As a result, the driving dynamics of the SimRod vehicle is assessed in the simulation environment and the stability of the vehicle in the turn with respect to the grip factor and vehicle speed is analyzed.

KEYWORDS: AMESim, Prescan, loss of stability, autonomous vehicle

1 Introduction

The decision to drive an autonomous vehicle will be made by a computer, so the physical limitations of such a vehicle must be known in advance. One such constraint is the limit of stability (reaching a skid) when such a vehicle goes around a curve.

The aim of this work was to find, through simulation, the limit state - the speed at which the SimRod vehicle loses stability. Different modelling software such as AMESim, MATLAB, ADAMS/Car and others can be used to simulate the driving dynamics of the vehicle. This paper deals with the simulation of the SimRod vehicle dynamics in AMESim, Simulink and Prescan, taking advantage of the features of all three programs due to the so-called co-simulation. For this type of use of the software, mutual data transfer and the use of interfaces is necessary.

Each of the mentioned software is suitable for some specific part of the problem. The AMESim software is used in this work to create the SimRod vehicle model. In the following chapter “Virtual model creation” the modelling of the SimRod vehicle in AMESim is discussed in more detail. A model is created, and values are assigned to it based on data from the real SimRod vehicle.

The environment in which the virtual simulation takes place is created in the Prescan software and is the topic of the chapter titled “Creating a driving maneuver”. In this software it is necessary to create an experiment - a driving scenario, which will contain a road to which different surfaces will be subsequently assigned. Several simulations will be carried out, modifying the road surface to provide different values of the coefficient of adhesion. The vehicle in this scenario must be able to move. The control of this vehicle is implemented through Simulink.

DOI: 10.2478/scjme-2022-0047, Print ISSN 0039-2472, On-line ISSN 2450-5471

Subsequently, co-simulation is performed through these three software. In it, the vehicle has to follow a desired trajectory with a certain speed. The speed is gradually increased with each succeeding experiment, and a limiting speed is found at which the SimRod vehicle skids.

2 Virtual model creation

The creation of the virtual model for the simulation of the cornering maneuver was carried out in AMESim, specifically in the 3D mechanics environment. An existing model in .cad format was imported into it, in which the links between the different components of the vehicle were created (Fig. 1). The parameters of the vehicle were inserted into the model, which were obtained from the Catia program (masses of the individual parts and moments of inertia). Subsequently, the entire model was generated on the AMESim workspace, where the vehicle's wheel drive, damping and steering were added to the generated schematic. A large number of rigid constraints were used to create a strong connection between the individual elements of the model. These rigid links were used because of the large number of degrees of freedom, since the space frame model was not uniform, and the entire vehicle system was computationally difficult.

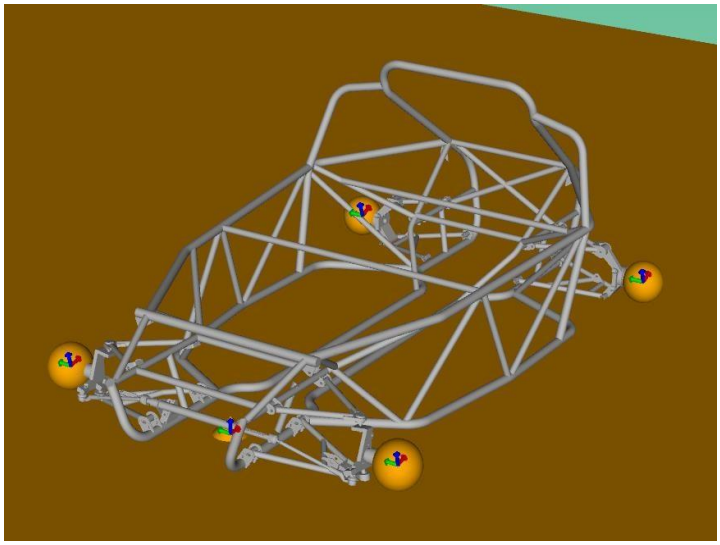


Fig. 1 SimRod virtual vehicle model created in 3D mechanics

The center of the whole assembly is the chassis. This model is the central module for vehicle dynamics modelling, to which all sub-models can be connected (damping - spring, shock absorber, stabilizer, tire, sensors, engine, brakes, steering system, external loads. The number of degrees of freedom (DOF) depends on the number of bodies and the type of connections between them. If we consider a multi-body chassis system with no connections between its parts, the model will have to have 60 degrees of freedom. The detailed classification of the degrees of freedom is given below.

- Body = 6 DOF
- Steering rod = 6 DOF
- Wheel mounting = 4x6 DOF
- Wheels = 4x6 DOF

There are several types of linkages between all subsystems and the body. It should be noted that kinematic linkages represent relative motion between bodies.

If we consider the complete relative motion between the body and the axle system then the coupling between the body and each wheel mount can be interpreted as a kinematic constant. This coupling is called the generalized suspension constant and, from a kinematic multibody

point of view, contains five degrees of freedom between the body and the wheel mount. The relative degree of freedom is the vertical travel of the wheel, labeled z_{rel} (Fig. 2)

The kinematic coupling between the steering (steering rod) and the body is a prismatic coupling with one degree of one degree of freedom. The degree of freedom represents the relative displacement between the steering and the body, labeled y_{crav} (Fig. 2)

The kinematic linkage between the wheel and the wheel mount is a rotary joint (one degree of freedom). The axis of the joint is oriented according to the axis of rotation of the wheel. The degree of freedom is the relative angle of rotation of the wheel with respect to the wheel mount, denoted as $\theta_{rel.}$ (Fig. 2)

By considering these linkages between the different parts of the mechanism for the number of degrees of freedom of such a vehicle is reduced. The mechanism described in this model operates with 15 degrees of freedom, namely: (Fig. 2)

- Body = 6 DOF
- Steering rod = 1 DOF
- Wheel mounting = 4x1 DOF
- Wheels = 4x1 DOF

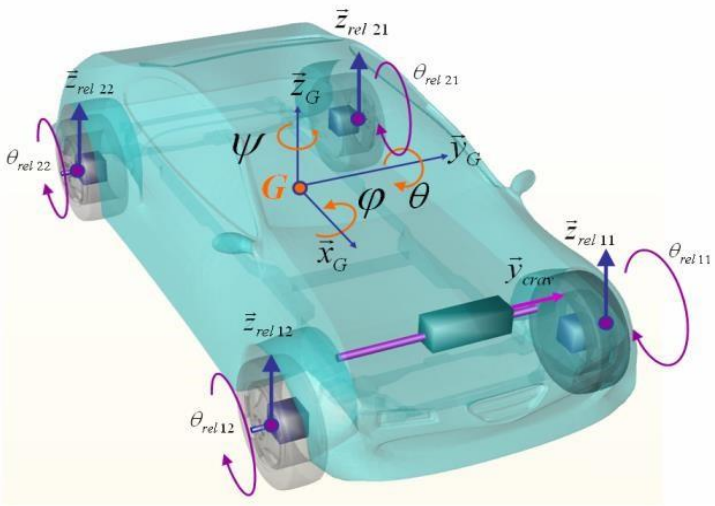


Fig. 2 Mechanism with 15 degrees of freedom

Such a 15 DOF vehicle model represents an actual physical SimRod vehicle. It is therefore necessary to assign values and parameters of this physical vehicle to the virtual model. These input parameters are:

- mass and moments of inertia:
- suspended part of the vehicle
- inertia of the sprung part of the vehicle
- mass and inertia of the front and rear wheel mounting
- mass and inertia of the front and rear wheels

Some of the input parameters can be seen in the figures Fig. 3 Fig. 4 Fig. 5.

Masses and inertias : carbody and rack

Mass of carbody (sprung mass)	kg	**600**
Carbody moment of inertia in X direction (sprung mass) - Carbody frame (R1)	kgm**2	**56.97**
Carbody moment of inertia in Y direction (sprung mass) - Carbody frame (R1)	kgm**2	**391.6**
Carbody moment of inertia in Z direction (sprung mass) - Carbody frame (R1)	kgm**2	**410.1**
Carbody product of inertia around XY direction (sprung mass) - Carbody frame (R1)	kgm**2	**-5.193**
Carbody product of inertia around XZ direction (sprung mass) - Carbody frame (R1)	kgm**2	**5.904**
Carbody product of inertia around YZ direction (sprung mass) - Carbody frame (R1)	kgm**2	**0.60095**
Mass of steering rack	kg	**2.07**

Fig. 3 Mass and moments of inertia of the chassis

Masses and inertias : Front left axle (11)

Front left axle (11) : mass of spindle	kg	**2.068**
Front left axle (11) : mass of wheel	kg	**18**
Front left axle (11) : Spindle : moment of inert...	kgm**2	**0.00221723**
Front left axle (11) : Spindle : moment of inert...	kgm**2	**0.00235031**
Front left axle (11) : Spindle : moment of inert...	kgm**2	**0.00221716**
Front left axle (11) : Spindle : product of inerti...	kgm**2	**3.046e-06**
Front left axle (11) : Spindle : product of inerti...	kgm**2	**1.3e-08**
Front left axle (11) : Spindle : product of inerti...	kgm**2	**5.84e-07**
Front left axle (11) : Wheel : moment of inerti...	kgm**2	**0.5**
Front left axle (11) : Wheel : moment of inerti...	kgm**2	**1**
Front left axle (11) : Wheel : moment of inerti...	kgm**2	**0.5**
Front left axle (11) : Wheel : product of inerti...	kgm**2	0
Front left axle (11) : Wheel : product of inerti...	kgm**2	0
Front left axle (11) : Wheel : product of inerti...	kgm**2	0

Fig. 4 Front axle mass and moments of inertia

Masses and inertias : Rear left axle (21)

Rear left axle (21) : mass of spindle	kg	**2.171**
Rear left axle (21) : mass of wheel	kg	**18**
Rear left axle (21) : Spindle : moment of inertia in X direction - Spindle frame	kgm**2	**0.00251412**
Rear left axle (21) : Spindle : moment of inertia in Y direction - Spindle frame	kgm**2	**0.00278204**
Rear left axle (21) : Spindle : moment of inertia in Z direction - Spindle frame	kgm**2	**0.0025142**
Rear left axle (21) : Spindle : product of inertia (XY) - Spindle frame	kgm**2	0
Rear left axle (21) : Spindle : product of inertia (XZ) - Spindle frame	kgm**2	0
Rear left axle (21) : Spindle : product of inertia (YZ) - Spindle frame	kgm**2	**4.514e-06**
Rear left axle (21) : Wheel : moment of inertia in X direction - Wheel frame	kgm**2	**0.5**
Rear left axle (21) : Wheel : moment of inertia in Y direction - Wheel frame	kgm**2	**1**
Rear left axle (21) : Wheel : moment of inertia in Z direction - Wheel frame	kgm**2	**0.5**
Rear left axle (21) : Wheel : product of inertia (XY) - Wheel frame	kgm**2	0
Rear left axle (21) : Wheel : product of inertia (XZ) - Wheel frame	kgm**2	0
Rear left axle (21) : Wheel : product of inertia (YZ) - Wheel frame	kgm**2	0

Fig. 5 Rear axle mass and moments of inertia

3 Creating a driving maneuver

With such a modelled vehicle with dynamics it is possible to simulate some driving maneuver. In order for such a simulation to take place, the vehicle, the environment, must be created and the vehicle control must be somehow handled. The creation of the dynamic vehicle model was done in AMESim. The environment in which the vehicle performs the driving maneuver was created in Prescan.

The path created in PreScan is the result of joining the road segments. The creation of the road is followed by the creation of the path. It is the path that represents the actual path on which the vehicle is moving. The creation of the path can be done in two ways: the path will copy the road profile, or the path will be added manually using points that the vehicle must pass through.

Creating a track

The path for the vehicle was relatively simple due to the difficulty of computation. The track was constructed from a straight two-lane road with a lane width of 3.5 m, which continued through a curve with a constant radius of 30 m and then was straight again. All segments of the road were in a horizontal plane, so that there was no road slope anywhere on the track. The modelled track can be seen in Fig. 6.

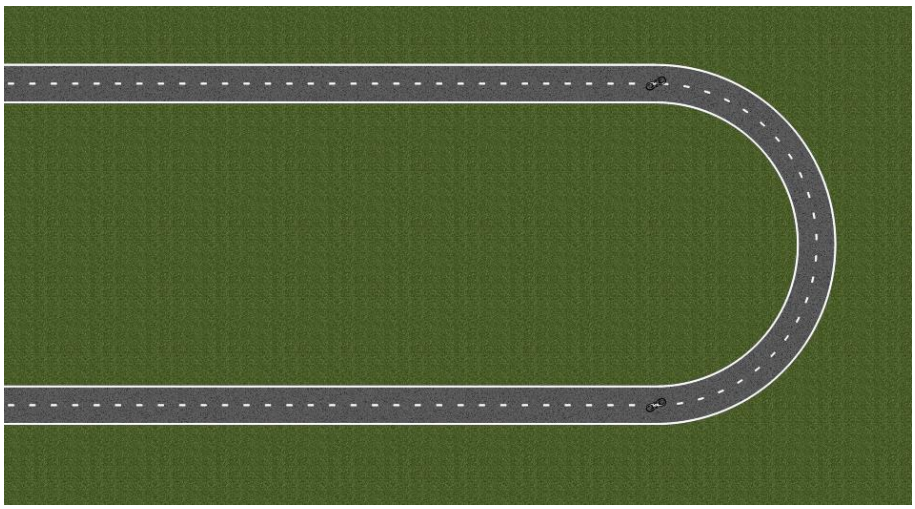


Fig. 6 Manoeuvre track

Vehicle control and speed profile

Vehicle control (steering, acceleration, braking) is performed in Simulink. In Prescan, the desired vehicle trajectory was defined on the track, which led through the center of the right lane. The controller's task was to calculate a steering command such that the vehicle would follow this trajectory as accurately as possible. A Stanley controller was used to steer the vehicle.

To control the longitudinal dynamics (acceleration, braking) a Stanley longitudinal driver was used. The input to it was the speed profile of the trajectory. The vehicle speed profile was set as a constant speed over the entire trajectory segment. This speed was in order to simulate the reaction in the wheels when going through the turns and whether the vehicle was stable in that section. The initial constant speed was chosen to be 10 m/s and was increased by 0.1 m/s for each additional iteration of the simulation. A close-up view of the SimRod vehicle during the simulation can be seen in the Fig. 7.



Fig. 7 Detailed view of the SimRod vehicle

4 Loss of stability testing methodology

The aim of the work is to simulate the loss of stability of a vehicle, whereby the speed at which the vehicle loses stability in a left-hand bend with a radius of 30 m and the vehicle skidding occurs is investigated. For the limiting speed, when the vehicle skidding already occurs in a horizontal turn, the equation is:

$$v_s = \sqrt{R\ g\ \mu_y} \tag{1}$$

where $\mu_y = \mu$ is the adhesion coefficient, R is the radius of the turn and g is the gravitational acceleration coefficient.

The value of the adhesion coefficient is mainly influenced by the road surface; when driving on wet roads, the tire profile must break the water film and push the water out of the track in order for the road to make contact with the tire. If the height of the water film is high and the speed of travel is also high, then the water is not drained quickly enough, and aquaplaning occurs. The different values of the coefficient of adhesion are shown in Tab. 1.

Tab. 1 Coefficient of adhesion for different road types

Road	Adhesion coefficient
Concrete (dry)	0.8 – 1.0
Concrete (wet)	0.5 – 0.8
Asphalt (dry)	0.8 – 0.9
Asphalt (wet)	0.5 – 0.7
Gravel (wet)	0.6
Snow (compress)	0.2
Ice	0.1

The loss of stability was detected as follows. The vehicle in the simulation was moved on the roadway with a certain value of the coefficient of adhesion, driven by a controller, in order to follow a predefined trajectory. The initial speed of this vehicle was set to 10 m/s, and then the simulation was repeated with a speed increment of 0.1 m/s as many times as necessary until the vehicle reached a skidding turn and thus lost stability. Subsequently, this speed was considered as the speed at which skidding occurs and was observed. The radius of the turn that the vehicle followed in the simulation was identical in all experiments and was set to R = 30 m.

5 Results of the simulation

The stability loss was analyzed at different adhesion factors for different road types; thus, several simulations were performed. The values of the adhesion coefficient were chosen from Tab. 1, where values for the following types of road surfaces were chosen:

- dry concrete $\mu_{dc} = 1$
- dry asphalt $\mu_{da} = 0.8$
- wet concrete $\mu_{wc} = 0.5$
- wet asphalt $\mu_{wa} = 0.4$

The first limiting velocity at which loss of stability occurs was found be for dry concrete with a coefficient of adhesion $\mu = 1$. The recorded velocity resulting from the simulation at

which stability was lost with this value of the coefficient of adhesion was 16.8 m/s. The lateral forces acting in the wheels represent the vertical axis of the graph and are shown in Fig. 8. The moment when the vehicle lost stability is indicated by the black line.

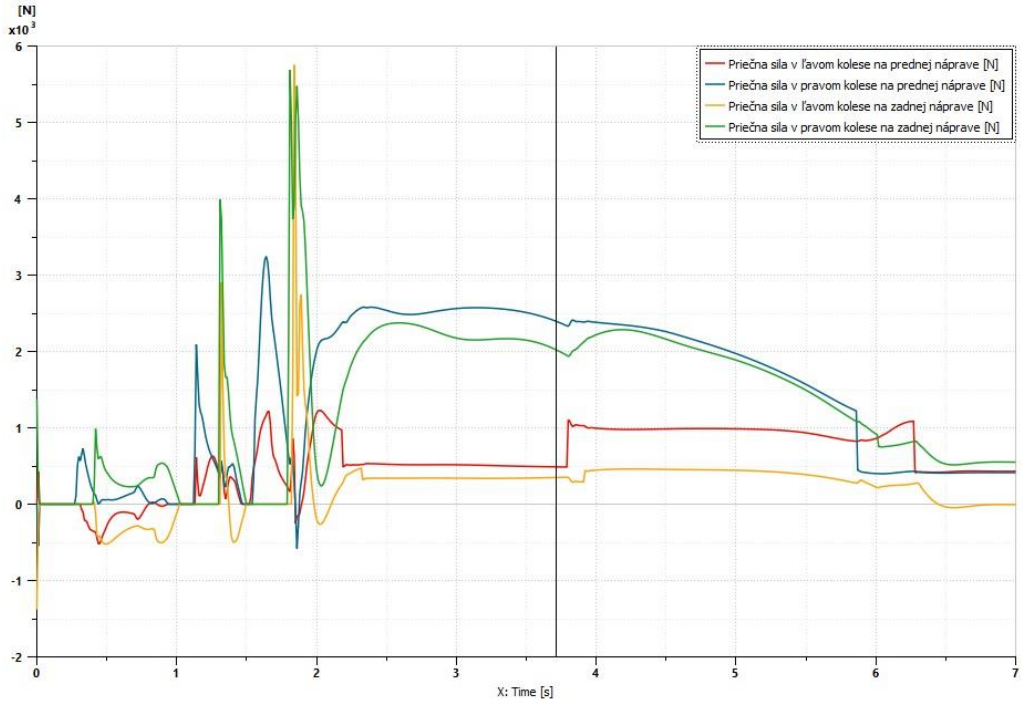


Fig. 8 Lateral forces on the wheels at a speed of 16.8 m/s

Fig. 8 shows the lateral forces at all wheels as they negotiate a left-hand bend. In the t = 3.8 *s*, it can be seen when the vehicle has lost stability. Loss of vehicle stability occurs when the centrifugal force of the vehicle is higher than the sum of the lateral forces in the wheels. The values of the lateral forces at the moment when the vehicle has lost stability on the road are given in Tab. 2

Tab. 2 Values of the lateral forces in the wheels during loss of stability at a speed of 16.8 m/s

Wheel	Lateral force (N)
Front right	2 329.84
Front left	1 102.4
Rear right	1 935.8
Rear left	351.6

The centrifugal acceleration of the vehicle through the turn was 8.66 ms^{-2}. Multiplying this acceleration by the mass of the vehicle m = 680 kg gives the centrifugal force of the vehicle. The centrifugal force in the lateral direction is then

$$F_y = m\,a = 680\ .\ 8.66 = 5963.6\ N \tag{2}$$

When stability is lost, the centrifugal force must be greater than the sum of the lateral forces in the wheels.

$$F_y > F_{FR} + F_{FL} + F_{RR} + F_{RL} \tag{3}$$

$$5963.6 > 2329.84 + 1102.4 + 1935.8 + 351.6$$

$$5963.6\ N > 5720.64\ N$$

For a dry asphalt roadway with a coefficient of adhesion μ = 0.8, a limiting skid speed of 15.1 *m/s* was found by simulation. The values of the lateral forces on the wheels are shown in Fig. 9.

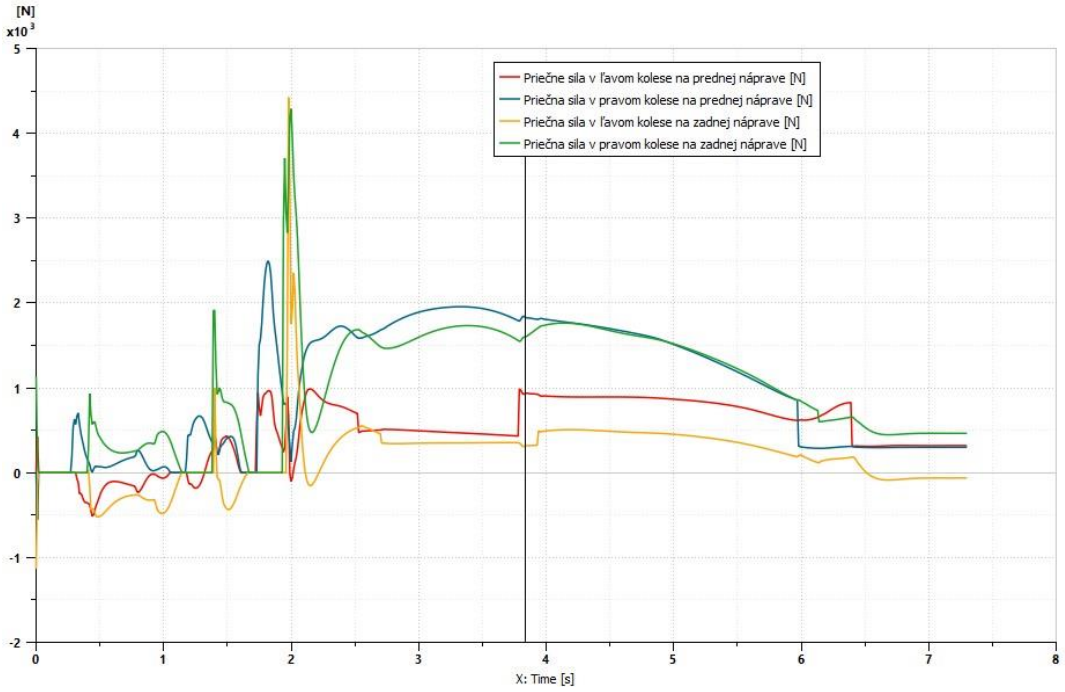


Fig. 9 Lateral forces on the wheels at a speed of 15.1 m/s

The values of the lateral forces at the moment when the vehicle has lost stability on the road are given in Tab. 3.

Tab. 3 Values of the lateral forces in the wheels during loss of stability at a speed of 15.1 m/s

Wheel	Lateral force (N)
Front right	1806.1
Front left	898.5
Rear right	1747.5
Rear left	499.6

The centrifugal acceleration of the vehicle at 15.1 *m/s* was 7.4 ms^2. To calculate the centrifugal force:

$$F_y = m\ a = 680\ .\ 7.4 = 5032\ N$$

$$F_y > F_{FR} + F_{FL} + F_{RR} + F_{RL}$$

$$5032 > 1806.1 + 898.5 + 1747.5 + 499.6 \quad (4)$$

$$5032\ N > 4951.7\ N$$

For a wet concrete roadway with a coefficient of adhesion μ = 0.5, a limiting skid speed of 12.7 *m/s* was found by simulation. The values of the lateral forces on the wheels are shown in Fig. 10.

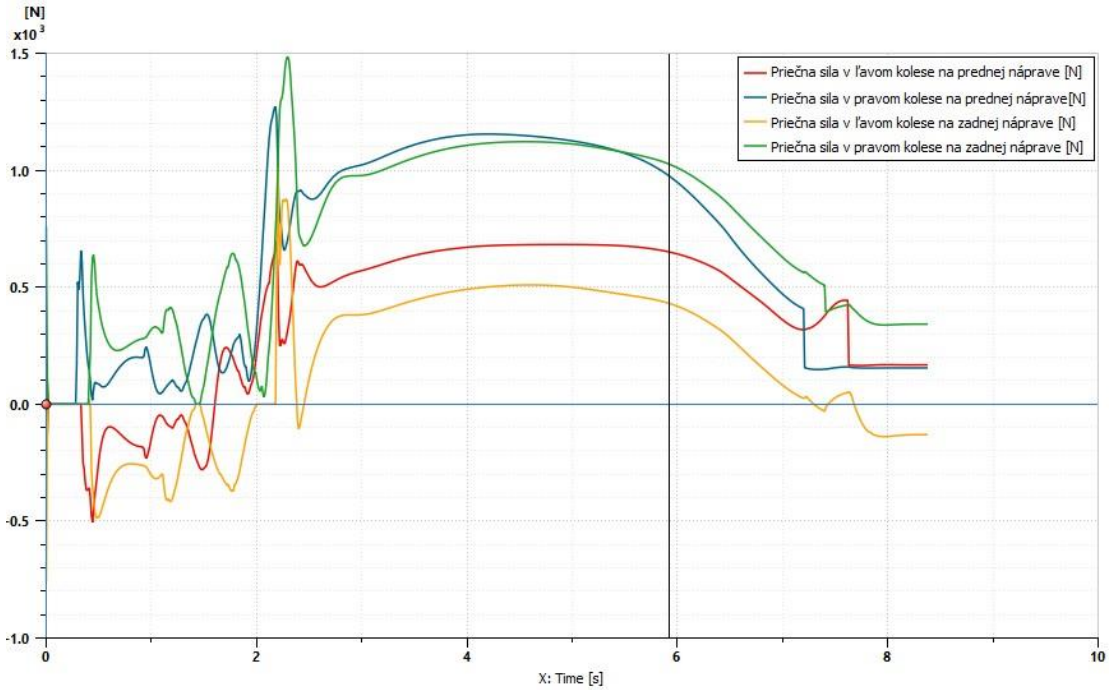


Fig. 10 Lateral forces on the wheels at a speed of 12.7 m/s

The values of the lateral forces at the moment when the vehicle has lost stability on the road are given in Tab. 4.

Tab. 4 Values of the lateral forces in the wheels during loss of stability at a speed of 12.7 m/s

Wheel	Lateral force (N)
Front right	1059.2
Front left	672.7
Rear right	1067.9
Rear left	461.8

The centrifugal acceleration of the vehicle at 12.7 *m/s* was 5.1 ms^{-2}. To calculate the centrifugal force:

$$F_y = m\,a = 680\ .\ 5.1 = 3468\ N$$
$$F_y > F_{FR} + F_{FL} + F_{RR} + F_{RL}$$
$$3468 > 1059.2 + 672.2 + 1067.9 + 461.8 \quad (5)$$
$$3468\ N > 3261.6\ N$$

For a wet asphalt roadway with a coefficient of adhesion μ = 0.4, a limiting skid speed of 11.4 *m/s* was found by simulation. The values of the lateral forces on the wheels are shown in Fig. 11.

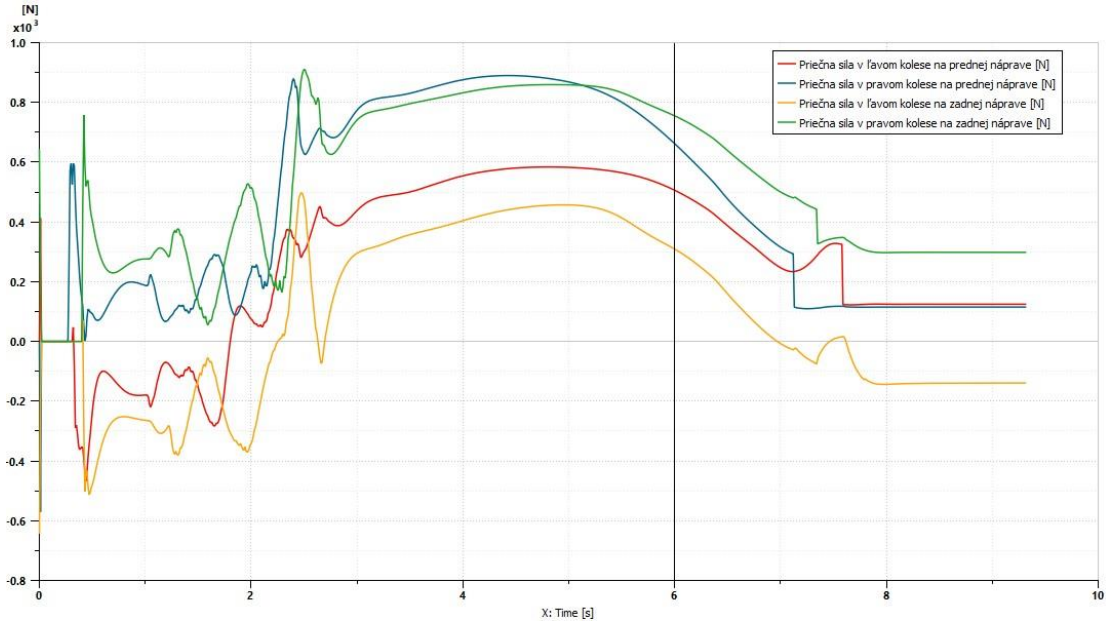


Fig. 11 Lateral forces on the wheels at a speed of 11.4 m/s

The values of the lateral forces at the moment when the vehicle has lost stability on the road are given in Tab. 5.

Tab. 5 Values of the lateral forces in the wheels during loss of stability at a speed of 11.4 m/s

Wheel	Lateral force (N)
Front right	762.8
Front left	552.6
Rear right	809.7
Rear left	387.2

The centrifugal acceleration of the vehicle at 11.4 *m/s* was 4.1 ms^{-2}. To calculate the centrifugal force:

$$F_y = m\,a = 680\ .\ 4.1 = 2788.1\ N$$

$$F_y > F_{FR} + F_{FL} + F_{RR} + F_{RL}$$

$$2788.1 > 762.8 + 552.6 + 809.7 + 387.2 \qquad (6)$$

$$2788.1\ N > 2512.3\ N$$

This section was concerned with finding the limiting speed for vehicle skidding in a corner for different coefficients of adhesion between the road and the tire. For the calculation of lateral stability in a horizontal turn, as mentioned above, Equation 1 holds. By taking the values R = 30 m and g = 9.81 $N.kg^{-1}$, we can calculate the limiting skidding speed through the turn for different values of the adhesion coefficient for different road surfaces. The table shows a comparison of the values of the velocity at which loss of stability occurs through simulation and also the calculated value using Equation 1.

Tab. 6 Comparison of vehicle limiting skidding speeds between simulation and theoretical calculations

Road type		Simulation values (m/s)	Calculated values (m/s)
Concrete	Wet	12.7	12.1
	Dry	16.8	17.2
Asphalt	Wet	11.4	10.8
	Dry	15.1	15.3

The maximum difference between the results obtained from the simulation and those calculated according to Equation 1 is 0.6 m/s, corresponding to 2.16 km/h. The simplified calculation and the simulation results are consistent with each other and therefore we assume that the simulation should be more accurate. However, it should be noted that the simulation shows smaller values compared to the simplified calculation but larger values on a dry surface.

CONCLUSION

The result of this work is a simulation of the driving of an autonomous vehicle SimRod where the aim was to determine the limit state in order to identify the behavior of the vehicle when driving through a turn with different surface i. e. the coefficient of adhesion was varied. The limit state of the vehicle on roads with different coefficient of adhesion was characterized and the limit speed at which the vehicle loses stability and skidding occurs was identified.

The vehicle that performs the experiment is modelled in the AMESim software. The different parts of the vehicle have their values (masses, moments of inertia, etc.) defined in it in order to work with the dynamics of that vehicle. The environment, i.e. the scenario in which the vehicle is travelling, is created in the Prescan software and consists of a two-lane road containing a turn with a radius of 30 m. The control of this vehicle is performed in Simulink software. The resulting simulation is a co-simulation of the three previously mentioned software.

The limiting speed of the vehicle at which the loss of stability occurs was detected on four different surfaces (Dry concrete, wet concrete, dry asphalt, wet asphalt). For each of these surfaces, a different coefficient of adhesion was defined in the simulation. For dry concrete, the coefficient of adhesion $\mu = 1$ was chosen and the limiting speed at which skidding occurred was 16.8 m/s. For wet concrete with $\mu = 0.5$, the limiting velocity was 12.7 m/s. For dry asphalt with $\mu = 0.8$, the limiting speed was found to be 15.1 m/s and for wet asphalt with $\mu = 0.4$, the vehicle lost stability at 11.4 m/s.

After verifying the results by calculations using the centrifugal force equations, it can be claimed that the results from the simulation are more accurate as they take into account several factors affecting the vehicle dynamics.

ACKNOWLEDGEMENT

This research was funded by Slovak Grant Agency APVV-19-0401, APVV-20-0428 and Slovak Research Agency ITMS+313011V334.

REFERENCES

[1] Urmson C, Anhalt J, Bagnell D, et al. "Autonomous driving in urban environments: Boss and the urban challenge", Journal of Field Robotics 25, pp. 425 – 466, **2008**.

[2] Saikia A, Mahanta C. "Vehicle stability enhancement using sliding mode based active front steering and direct yaw moment control", In: Control Conference (ICC), 2017 Indian pp. 378 – 384, **2017**.

[3] Yoshida, M, Nonaka, K., Sekiguchi, K. "Model predictive vehicle control with side slip angle restriction with suppression of modeling error by sliding mode control", In: Control Applications (CCA), 2014 IEEE Conference on 2014, pp. 328 – 333, **2014**.

[4] Rajamani R. "Vehicle dynamics and control", Springer Science & Business Media, **2011**.

[5] Jacobson, B.() Vehicle Dynamics. Compendium for course MMF062. Chalmers University of Technology2016

[6] Vlk, F. "Dynamika motorových vozidiel", Prof. Ing. František Vlk, DrSc., nakladatelsví a vydavatelství, 2003. ISBN 80-239-0024-2 (in Slovak)

[7] D. Zhang, X. Zeng, P. Wang, Q. Wang, "Co-simulation with AMESim and MATLAB for differential dynamic coupling of Hybrid Electric Vehicle", 2009 IEEE Intelligent Vehicles Symposium, pp. 761 – 765, **2009**. DOI: 10.1109/IVS.2009.5164373

[8] "Siemens Product Lifecycle Management Software Inc. Simcenter AMESim: Delivering engineering innovation with system simulation", **2018**. [online] Available at: https://feacomp.com/wp-content/uploads/2020/07/1.Simcenter-Amesim-Brochure_compressed.pdf.

[9] TASS Inernational: A Siemens Business, PreScan: Product overview, **2020**. [online]. Available at: https://tass.plm.automation.siemens.com/prescan-overview.

[10] Li, Z., Wang, P., Liu, H., Hu, Y., Chen, H. "Coordinated longitudinal and lateral vehicle stability control based on the combined-slip tire model in the MPC framework", Mechanical Systems and Signal Processing 161, **2021**. DOI: 10.1016/j.ymssp.2021.107947

[11] Lehotzký, P., Janeba, M., Galinski, M., Šoltés, L. "Testing the Readiness of Slovak Road Infrastructure for the Deployment of Intelligent Transportation", Strojnícky časopis – Journal of Mechanical Engineering 72 (2), pp. 103 – 112, **2022**. DOI: 10.2478/scjme-2022-0020